

# Maximum likelihood ADC parameter estimates improve selection of metastatic cervical nodes for patients with head and neck squamous cell cancer

Nikolaos Dikaïos<sup>1</sup>, Shonit Punwani<sup>2</sup>, Valentin Hamy<sup>1</sup>, Pierpaolo Purpura<sup>2</sup>, Heather Fitzke<sup>3</sup>, Scott Rice<sup>2</sup>, Stuart Taylor<sup>3</sup>, and David Atkinson<sup>3</sup>

<sup>1</sup>Department of Medical Physics and Bioengineering, University College London, London, Greater London, United Kingdom, <sup>2</sup>Department of Radiology, University College London Hospital, <sup>3</sup>Centre for Medical Imaging, University College London

**Purpose:** The aim of this work was to determine whether classification of benign and metastatic cervical nodes based on diffusion weighted imaging (DWI) could be improved by use of a maximum likelihood algorithm for derivation of ADC parameters. A non linear least squares (LSQ) algorithm is usually used to fit parameters to the measured MR signal intensities as a function of b-value. LSQ assumes that the noise in high b-values is normally distributed whereas in reality it follows a Rice distribution. To account for the Rician noise, maximum likelihood (ML) algorithms have been proposed [1] that provide unbiased ADC estimates. In this work the monoexponential, stretched exponential and biexponential models were examined, with their involved parameters calculated using the LSQ and the ML algorithms.

**Method:** Axial diffusion weighted images of the neck were acquired using a STIR-EPI DWI sequence on a 1.5T Siemens Avanto for 16 patients with histological confirmed unilateral cervical nodal metastases from head and neck squamous cell carcinoma. Trace diffusion weighted images were derived at b=0 and b= 50, 100, 300, 600, 1000 s/mm<sup>2</sup>. Solid components of the metastatic and the largest contralateral benign nodes were contoured on b=300 images by two radiologists in consensus. Benign and metastatic contours were transferred onto ML and LSQ derived parametric maps for each model (i.e. the heterogeneity index (a-map) and ADC (ADC<sub>se</sub>) of a stretched exponential [2]; the ADC of a monoexponential (ADC<sub>me</sub>); the perfusion fraction (f-map), the perfusion sensitive ADC (ADC<sub>fast</sub>) and the ADC (ADC<sub>slow</sub>) of a biexponential model [3]). As 6 b-values is not sufficient (<10) to reliably perform a biexponential fit [4]; ADC<sub>fast</sub> (monoexponential fit of b=0, 50 and 100), ADC<sub>slow</sub> (monoexponential fit of b=300, 600 and 1000) estimates were used as constants for the biexponential model enabling derivation of the f-map. A paired t-test was used to compare mean ML and LSQ derived parameter values in both benign and metastatic nodal groups. The mean parametric values were also used as input variables to build separate linear discriminant analysis (LDA) models from ML and LSQ datasets. Receiver operator characteristic (ROC) area under curve (AUC) was calculated for ML and LSQ models allowing comparison of performance for classification of benign and metastatic nodes. The mean AUC of 1000 sub-samples (Bootstrapping) for both models was also calculated. Leave-one-out cross validation (LOO) was performed to assess the accuracy of both models for independent samples.

**Results:** ML derived ADC<sub>me</sub>, ADC<sub>slow</sub> estimates were larger and f-map values smaller than LSQ estimates for benign and metastatic nodes (table I). There was also a small but significant difference between ML and LSQ estimates of ADC<sub>se</sub> for metastatic nodes (table I). The ROC AUC for prediction of metastatic nodal status of the ML was higher than the LSQ for both the original and the bootstrapped sample (table II). The ML derived model classified 75% and the LSQ model 62% of nodes correctly using LOO cross validation of independent samples (figure 2).

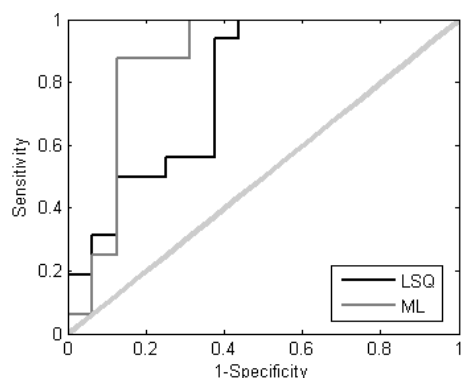


Figure 1: ROC curves of the LSQ and ML predictive models for the original dataset.

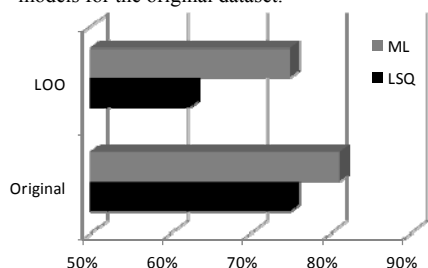


Figure 2: Percentage of correct classifications of the ML and LSQ predictive model for the original and LOO dataset.

Table I: Comparison of the mean parametric values between LSQ and ML estimates; significant difference at p<0.05 level.

	Benign cervical node			Metastatic cervical node		
	LSQ	ML	p-value	LSQ	ML	p-value
ADC <sub>me</sub>	1.0190	1.2226	0.0262	0.9290	0.9902	1.65E-07
ADC <sub>slow</sub>	1.0087	1.0881	0.0001	0.9235	0.9644	1.12E-07
ADC <sub>fast</sub>	2.2680	2.2380	0.2141	1.5927	1.5867	0.6541
f-map	0.1865	0.1056	7.33E-10	0.1447	0.0655	3.31E-11
ADC <sub>se</sub>	1.1240	0.9936	0.3204	0.8565	0.8502	0.0081
a-map	0.7040	0.7055	0.6934	0.7775	0.7747	0.2145

Table II: AUC of the ROC curves for the original and the resampled dataset. CI is the confidence interval.

Asymptotic 95% CI				
	AUC	Std. Error	Lower Bound	Upper Bound
<b>ML</b>				
Original	0.8711	0.0726	0.7288	1.0000
Bootstrap	0.8708	0.0724	0.7373	0.9843
<b>LSQ</b>				
Original	0.7852	0.0829	0.6228	0.9476
Bootstrap	0.7883	0.0839	0.6358	0.9140

**Conclusions:** Mean diffusion related parametric values were found to be significantly different for ML and LSQ algorithms. For high SNR the noise distribution of the MR signal is normal, hence the ADC<sub>fast</sub> that is calculated from early b-values is not significantly different for the two algorithms. The predictive model that was based on ML estimated mean parametric values has larger AUC for both the original and the resampled dataset than the one based on LSQ. The two models were evaluated with leave-one-out cross validation and the ML model classified the observations more accurately than the LSQ model. Our results support the use of a ML over LSQ algorithm where quantitative DWI parametrics are applied to the classification of clinical states. .

**References:** [1]Walker-Samuel S et al, Robust estimation of the apparent diffusion coefficient (adc) in heterogeneous solid tumors MRM 62(2):420-9 [2] Bennett KM et al Characterization of continuously distributed cortical water diffusion rates with a stretched-exponential model MRM 50(4):727-34 [3]Le Bihan D et al Separation of diffusion and perfusion in intravoxel incoherent motion MR imaging Radiology 168(2):497-505 [4] Lemke A et al Toward an optimal distribution of b values for intravoxel incoherent motion imaging Magn Reson Imaging 29(6):766-776.